

Slovenská technická univerzita v Bratislave
Stavebná fakulta

Ing. Matej Medľa

Autoreferát dizertačnej práce

**SOLVING PARTIAL DIFFERENTIAL EQUATIONS
USING FINITE VOLUME METHOD
ON NON-UNIFORM GRIDS**

na získanie akademického titulu *philosophiae doctor (PhD.)*
v doktorandskom študijnom programe
9.1.9 Aplikovaná matematika

Bratislava 2018

Dizertačná práca bola vypracovaná v dennej forme doktorandského štúdia na Katedre matematiky a deskriptívnej geometrie SvF STU v Bratislave.

Predkladateľ: Ing. Matej Medľa
Katedra matematiky a deskriptívnej geometrie
SvF STU, Bratislava

Školiteľ: Prof. RNDr. Karol Mikula, DrSc.
Katedra matematiky a deskriptívnej geometrie
SvF STU, Bratislava

Oponenti: prof. RNDr. Daniel Ševčovič, DrSc.
Katedra aplikovanej matematiky a štatistiky
FMFI UK, Bratislava

doc. Ing. Gabriel Okša, PhD.
Matematický ústav
SAV, Bratislava

doc. RNDr. Zuzana Krivá, PhD.
Katedra Matematiky a Deskriptívnej Geometrie
SvF STU, Bratislava

Autoreferát bol rozoslaný dňa

Obhajoba dizertačnej práce sa koná dňa o hod. na Katedre matematiky a deskriptívnej geometrie SvF STU v Bratislave, Radlinského 11.

prof. Ing. Stanislav Unčík, PhD.
dekan Stavebnej fakulty

Abstract

This thesis deals with a finite volume method on non-uniform 2D quadrilateral and 3D hexahedral meshes.

In the first part we deal with a construction of such meshes for discretization of 2D surfaces and 3D computational domains. The main tool for grid construction is a surface evolution. In the case of the construction of hexahedron mesh a quadrilateral mesh is evolved through the 3D computational domain. In the resulting mesh a time dimension is understood as a third spatial dimension. Then a method for quadrilateral remeshing of a triangulated surface is developed. The initial quadrilateral surface evolves in a suitably designed vector field to the given triangulated surface. In both applications the surface evolutions are accompanied by a tangential redistribution of points to achieve more uniform meshes.

In the second part we solve the partial differential equations on 3D grids constructed by our methods. First, we suggest new method for solution of the geodetic boundary value problem on hexahedron meshes, i.e. we solve the Laplace equation inside a domain and the oblique derivative condition on a boundary. This oblique derivative boundary condition can be understood as a stationary advection equation and we design a method for its discretization based on higher order upwind principle. Then we present a novel second order inflow-implicit/outflow-explicit scheme for solving an advection equation on non-uniform meshes. For all mathematical models we present numerical experiments showing their order of convergence and further properties related to applications.

keywords: finite volume method, surface evolution, mesh construction, non-uniform meshes, oblique derivative, advection equation, Laplace equation

Abstrakt

Táto záverečná práca sa venuje metóde konečných objemov pre nerovnomerné 2D štvoruholníkové a 3D šesťstenové (hexahedrálne) siete.

V prvej časti práci prezentujeme postupy na výrobu discretizácie plôch a tvorbu trojrozmerných výpočtových sietí. Hlavná myšlienka spočíva vo vývoji plôch. V prípade 3D hexahedrálnych sietí je vyvíjaná 2D štvoruholníková sieť vo vnútri 3D výpočtovej oblasti. Vo výslednej hexahedrálnej sieti je časový rozmer chápaný ako tretí priestorový rozmer. Vrcholy šesťstenovej siete sú dané diskretnými bodmi vyvíjajúcej sa plochy v diskretných časových intervaloch. V ďalšej časti sa venujeme takzvanému remeshingu trojuholníkovej siete na štvoruholníkovú. Počiatočná štvoruholníková sieť je vyvíjaná vo vektorovom poli smerom k trojuholníkovej sieti. V oboch prípadoch je použitá redistribúcia bodov plochy na dosiahnutie rovnomernejšej diskretizácie.

Druhá časť práce sa venuje riešeniu geodetickej okrajovej úlohy na nami vytvorených trojrozmerných sieťach. Z matematického pohľadu to znamená riešiť Laplaceovu rovnicu s predpísanou šikmou deriváciou na jej hranici. Predpísaná šikmá derivácia sa dá chápať ako stacionárna rovnica advekcie. V práci prezentujeme novú metódu vyššieho rádu na riešenie rovnice advekcie, ktorá je založená na upwind metóde. Ďalej prezentujeme novú inflow-implicit/outflow-explicit metódu druhého rádu na riešenie nestacionárnej rovnice advekcie na nerovnomerných sieťach. Pre všetky matematické modely prezentujeme numerické experimenty ukazujúce rád konvergence a možnosti ich aplikácií.

klúčové slová: metóda konečných objemov, vývoj plôch, tvorba siete, nerovnomerné siete, šikmá derivácia, rovnica advekcie, Laplaceova rovnica

Contents

1	Introduction	4
1.1	Lagrangian Evolution Model	4
1.2	Tangential redistribution of points	5
1.2.1	Area-based redistribution	6
1.2.2	Angle-based redistribution	6
2	Construction of the 3D computational grid	7
2.1	Numerical scheme	7
3	Tri-to-quad remeshing	8
3.1	Evolution of the surface	9
3.2	Numerical experiments	10
3.2.1	Example 2: Different resolutions	11
4	Gaussian curvature based redistribution	12
5	Geodetic boundary value problem	12
5.1	Discretization of oblique derivative BVP	13
5.1.1	Approximation of the Laplace equation	13
5.1.2	Approximation of the oblique derivative boundary condition	14
5.2	Numerical experiments	15
6	Advection equation	15
7	Conclusions	17
	References	18
	Zoznam publikačnej činnosti	19

1 Introduction

From the times of Isaac Newton and Gottfried Wilhelm Leibniz partial differential equations (PDE) are the fundamental tool to solve problems in a modern science. The most of the complex problems can not be solved by an analytical methods. This thesis deals with the finite volume method (FVM) for solving PDEs and its several applications.

It is divided into two part. The first part deals with a creating a non-uniform 2D surface and 3D volume grids based on a novel approach of the surface evolution.

The first type of a mesh is a 3D mesh for the geodetic boundary value problem (GBVP). Computational domain for such a problem is a region over a local Earth topography. The Earth surface is evolved through the 3D computational domain and the 3D grid points are taken as a time-spatial discrete points of the evolving surface. The 2D surface mesh generation deals with a problem of remeshing a triangulated surface into the quadrilateral mesh. The method is inspired by a level set approach to a surface reconstruction from a point cloud. This approaches evolve a level set function in a vector field that is a gradient of the distance function of the point cloud. We suggest a similar method for a Lagrangian surface evolution utilizing these principles.

In the rest of the thesis we are dealing with finite volume methods on non-uniform hexahedron meshes constructed by the method presented in the first part of the thesis. First we deals with solving the geodetic boundary value problem. Mathematically it is a Laplace equation with an oblique derivative boundary condition. Oblique derivative boundary condition is given by a prescribed value of a derivative of the unknown T in the direction of the vector \mathbf{v} on the boundary. This can be written in the form $\nabla T \cdot \mathbf{v} = g$. This can be understood as a stationary advection equation for which we suggest a novel higher order upwind scheme. At last we deal with a non-stationary advection equation utilizing the oblique derivative boundary condition discretization from GBVP. We also propose an improved second order method with more accurate approximations.

1.1 Lagrangian Evolution Model

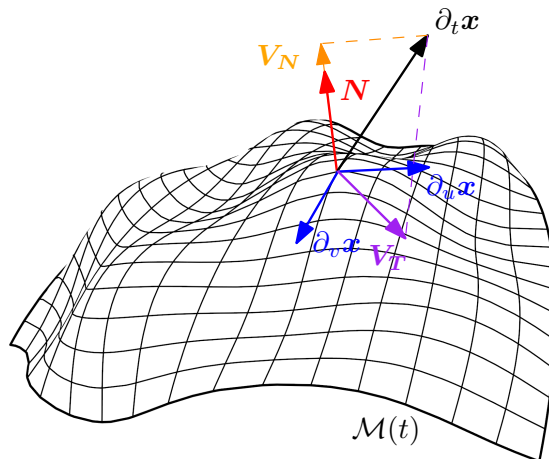
Let us consider a family of parametric surfaces $\mathcal{M}(t) = \{\mathbf{x}(t, u, v) | (u, v) \in [0, 1]^2, t \in [0, t_{end}]\}$ obtained by evolving in a time t an initial surface $\mathbf{x}(0, \cdot, \cdot) = S$. The evolution is driven by the following partial differential equation [6]

$$\begin{aligned} \frac{\partial \mathbf{x}}{\partial t} &= \mathbf{V}_N + \mathbf{V}_T = \beta \mathbf{N} + \mathbf{V}_T \\ \mathbf{x}(0, \cdot, \cdot) &= S, \end{aligned} \tag{1}$$

where \mathbf{V}_T is the evolution in tangential direction.; and \mathbf{V}_N represents the evolution by speed β in the outward unit normal direction \mathbf{N} to the surface. The component in the normal direction \mathbf{V}_N affects the surface image, while, at least in the continuous settings, \mathbf{V}_T has no impact on the surface image.

In both of the applications, the 3D grid construction and 2D surface remeshing, the surface evolution model is influenced by a mean curvature term so the evolution in the direction of the normal can be rewritten as

$$\beta \mathbf{N} = H \mathbf{N} + f \mathbf{N}, \tag{2}$$

Figure 1: Image of the surface $\mathcal{M}(t)$ and the normal and tangent vectors

where $H\mathbf{N}$ is the mean curvature vector.

Let us define a local area density

$$g = |\partial_u \mathbf{x} \times \partial_v \mathbf{x}| = \sqrt{\det \begin{bmatrix} \partial_u \mathbf{x} \cdot \partial_u \mathbf{x} & \partial_u \mathbf{x} \cdot \partial_v \mathbf{x} \\ \partial_v \mathbf{x} \cdot \partial_u \mathbf{x} & \partial_v \mathbf{x} \cdot \partial_v \mathbf{x} \end{bmatrix}}. \quad (3)$$

The local area density represents a density of points along the surface. In the quad approximation of the surface, g is related to the size of the finite volumes. Bigger value of the local area density means smaller finite volumes and vice-versa. Finite volumes are composed of quads, see the Figure 2. This quantity is used to control the area of the finite volumes thus indirectly control the area of the quads.

1.2 Tangential redistribution of points

The surface evolution model (1) for both of the applications is accompanied by a redistribution of points along the surface. This term is given in the equation (1) by a vector \mathbf{V}_T . Because of different nature of both applications, we use different redistributions.

For a computational domain over the Earth topography the surface can be understood as a mesh of intersected curves, meridians and parallels. In this case we use a redistribution of points relative to the curves (parallels and meridians) that the surface is composed of. This redistribution leads to a uniform distribution of points along parallels and meridians.

For a quadrilateral mesh generated by remeshing of a triangulated mesh we use the area redistribution. In this case the image of the initial surface is significantly changing in time and the angle redistribution is necessary for a good quality output, too.

To this aim the tangential component in (1) is defined as

$$\mathbf{V}_T = \mathbf{V}_T^r + \mathbf{V}_T^n \quad (4)$$

where the vector \mathbf{V}_T^r contributes to the quad area size control and the vector \mathbf{V}_T^n handles the control of the angles of the quads. In general \mathbf{V}_T^n can be any tangential movement.

1.2.1 Area-based redistribution

We are interested in the evolution of g given by (3) with respect to the normal and tangential velocities in (1). We want the surface area density g to converge to a prescribed area density c . A one useful prescribed density c is a constant density resulting in a uniform quad sizes of a discretized surface. In that case we chose

$$c(u, v) = A. \quad (5)$$

Another useful prescribed density c is a density depended on a Gaussian curvature $G(u, v)$. This results in more dense quad mesh in the areas of high Gaussian curvature. One possibility is to take a function \hat{c} defined as

$$\hat{c}(u, v) = 1 / \left(p \max \left(\frac{|G(u, v)|}{G_{cut}}, 1 \right) + 1 \right), \quad (6)$$

where p and G_{cut} are chosen values. In a discrete surface this means that quads with a Gaussian curvature greater then G_{cut} will be $p+1$ times greater then the quads with a zero Gaussian curvature. For a valid area density it holds that its surface integral is equal to the area of the surface. This is satisfied by normalizing the function \hat{c} ,

$$c(u, v) = A \frac{\hat{c}(u, v)}{\int_0^1 \int_0^1 \hat{c} \, dudv}. \quad (7)$$

A relation between \mathbf{V}_T and g that satisfies leads to a prescribed area density c is summarized in Corollary 1 in terms of the Laplace-Beltrami operator [6].

Corollary 1. *Let us assume that \mathbf{V}_T^r is a gradient vector field of a potential φ . Then $\mathbf{x}(t, \cdot)$ evolves to a surface with area density c if the Laplace-Beltrami operator applied on the the function φ satisfies the following relation*

$$\Delta_{\mathbf{x}} \varphi = \nabla_{\mathbf{x}} \cdot \nabla_{\mathbf{x}} \varphi = -\nabla_{\mathbf{x}} \cdot \mathbf{V}_T^n + H\beta - \frac{1}{A} \iint_{\mathcal{M}} H\beta \, d\mathcal{M} + \left(\frac{c}{g} - 1 \right) \omega_r. \quad (8)$$

By imposing only the Neumann boundary condition for an open surface problem, (8) attains infinitely many solutions which differ only by a constant, thus the gradient $\mathbf{V}_T^r = \nabla_{\mathbf{x}} \varphi$ is naturally the same for each solution. However, a unique solution for (8) can be obtained by imposing a Dirichlet boundary condition at one point of \mathcal{M} .

1.2.2 Angle-based redistribution

A purpose of this redistribution is to control the angles of quadrilaterals that are composing the surface. Let us assume that the surface is divided into quadrilateral patches. In the discrete settings these patches are represented by the quads which compose the surface. The angle redistribution is directly dependent on the vectors $\partial_u \mathbf{x}$ and $\partial_v \mathbf{x}$. Let $\mathbf{x}_i, i = 1, \dots, n$ be a corner point of quadrilateral patch and n be the number of all corner points of quadrilateral patches on the surface. Let $N_{\square}(\mathbf{x}_i)$ be a set of quadrilateral patches that contain \mathbf{x}_i and let $\#N_{\square}(\mathbf{x}_i)$ be its cardinality. Let $\partial_u \mathbf{x}^j, \partial_v \mathbf{x}^j$ be the tangent vectors of the j -th neighboring quadrilateral patch.

At each corner point $\mathbf{x}_i, i = 1, \dots, n$ the angle-based tangential velocity \mathbf{V}_T^n is constructed as

$$\mathbf{V}_T^n = \text{proj}_T \left(\frac{\omega_n}{\#N_{\square}(\mathbf{x}_i)} \sum_{j \in N_{\square}(\mathbf{x}_i)} \left(1 + \frac{\partial_u \mathbf{x}^j}{|\partial_u \mathbf{x}^j|} \cdot \frac{\partial_v \mathbf{x}^j}{|\partial_v \mathbf{x}^j|} \right) (\partial_u \mathbf{x}^j + \partial_v \mathbf{x}^j) \right). \quad (9)$$

Formula (9) utilizes the fact that the cosine of angle between two vectors can be computed as the inner product $(\partial_u \mathbf{x}/|\partial_u \mathbf{x}|) \cdot (\partial_v \mathbf{x}/|\partial_v \mathbf{x}|)$ and such weights are forced to be positive using the shift by 1. Intuitively, in case of an acute angle, moving \mathbf{x}_i in direction $\partial_u \mathbf{x} + \partial_v \mathbf{x}$ enlarges the angle between $\partial_u \mathbf{x}$ and $\partial_v \mathbf{x}$. As the resulting vector does not have to lie in the tangent plane, we project it on the tangent plane utilizing $\text{proj}_T(\mathbf{V}) = \mathbf{V} - (\mathbf{V} \cdot \mathbf{N})\mathbf{N}$. S

2 Construction of the computational grid above the Earth topography

Let Ω be a 3D domain bounded by a boundary $\partial\Omega$, which is composed of several parts. The first part of the boundary $\partial\Omega$ represents an approximation of the Earth surface. The second one is given by an approximation of chosen satellite orbit at the height h . Further two boundaries are given by planes going through two meridians and the last two boundaries are given by planes going through two parallels

The main idea is to evolve the initial surface (Earth topography) through the 3D computational domain and then take the discrete points of the surface in discrete time intervals and use them as vertices of a 3D mesh. Using this evolution we achieve that the surface continuously forms a shape of a part of the ellipsoid and the mathematical formulation of this process is given by

$$\partial_t \mathbf{x}(u, v, t) = \varepsilon (H\mathbf{N} + f\mathbf{N}). \quad (10)$$

where the mean curvature term H is smoothing the evolution. The scalar ε is a parameter determining how fast the surface is moving.

We are going to use a redistribution of points according to the curves forming the surface. These individual curves can be seen as “deformed” meridians and parallels. The Earths surface can be parameterized such that $\mathbf{x}(u, \cdot)$ is the u -th meridian and $\mathbf{x}(\cdot, v)$ is the v -th parallel.

2.1 Numerical scheme

We adapt the finite volume approach, while a semi-implicit scheme is considered in time to linearize the Laplace-Beltrami operator and other non-linear terms in (1) in form (10).

The finite volume method assumes in general that the continuous surface \mathcal{M} is approximated by the union of so-called *control volumes* V_i , see Figure 2. We approximate quad using a bilinear interpolation.

Let us introduce the local vertex and quad indexing in the barycentric control volume V_i around vertex \mathbf{x}_i . The local vertex indices in a quad, see Figure 2, are denoted by $\mathbf{x}_j^k, k \in \{0, \dots, 3\}$, with $\mathbf{x}_j^0 = \mathbf{x}_i$, where j is a local index of quad. For a readability we are omitting the index i in a local indexing.

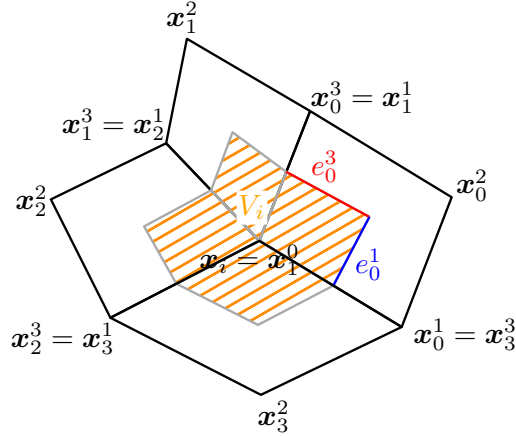


Figure 2: Finite volume V_i (shaded orange area) with local indexing of quad vertices and edges.

Utilizing a Green's theorem and bilinear interpolation on quads we approximate Laplace-Beltrami operator by

$$\int_{\partial V_i} \nabla_{\mathbf{x}} \mathbf{x} \cdot \mathbf{n} \, ds \approx \sum_{j \in N_{\square}(\mathbf{x}_i)} \frac{m(e_j^1)}{|N_j^1|} \left[\frac{1}{4} (-3\mathbf{x}_j^0 + 3\mathbf{x}_j^1 - \mathbf{x}_j^2 + \mathbf{x}_j^3) - \frac{a_j^1}{2} (-\mathbf{x}_j^0 - \mathbf{x}_j^1 + \mathbf{x}_j^2 + \mathbf{x}_j^3) \right] + \frac{m(e_j^3)}{|N_j^3|} \left[\frac{1}{4} (-3\mathbf{x}_j^0 - \mathbf{x}_j^1 + 3\mathbf{x}_j^2 + \mathbf{x}_j^3) - \frac{a_j^3}{2} (-\mathbf{x}_j^0 + \mathbf{x}_j^1 - \mathbf{x}_j^2 + \mathbf{x}_j^3) \right]. \quad (11)$$

The numerical experiments performed on the meshes generated by this method are presented in the part of the thesis that deals with a GBVP.

3 Remeshing a triangulated mesh into the quad mesh

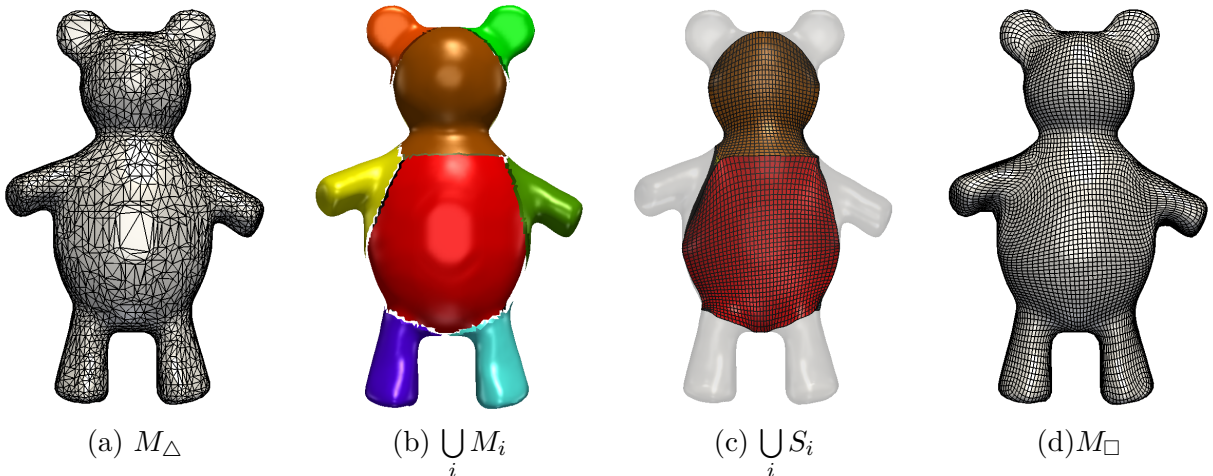


Figure 3: The fundamental steps of the proposed method: (a) Input mesh M_{Δ} ; (b) Patch layout; (c) Topology-Skeleton S ; (d) Resulting pure quadrilateral mesh M_{\square}

Another application for construction of a quad mesh is remeshing an object represented by a triangulated mesh into the quad mesh. Quad mesh is a mesh made of quadrilaterals. We introduce a method that takes as an input an object and its patch layout and output a quadrilateral mesh. A

patch layout is defined as partition of the surface into non-overlapping patches. The main principle of our method is in the evolution of quad mesh (initial condition) in the gradient of the distance function of the triangulated mesh. Such an evolution drives the quadrilateral mesh to the triangulated mesh. In this thesis we introduce a new approach to automatically generate a quadrilateral mesh on a surface \mathcal{M} preserving its patch layout structure. In particular, given a 3D shape \mathcal{M} represented by an unstructured closed triangle mesh M_Δ , we construct a pure quad mesh M_\square . We utilize a similar principles that are used for a level set reconstruction of the surface from the point cloud [7].

The overall process consists of three main phases summarized in Algorithm **Surface-Patch Quadrangulation** and illustrated in Figure 3.

algorithm: Surface-Patch Quadrangulation	
<hr/>	
Input:	Triangular Mesh M_Δ , quad edge length h
Output:	Pure Quadrilateral Mesh M_\square
1	$\{M_i\}_{i=1}^K \leftarrow \text{Mesh_Partitioning}(M_\Delta)$
2	$\{S_i\}_{i=1}^K \leftarrow \text{Topology_Skeleton}(\{M_i\}_{i=1}^K, h)$
3	$M_\square \leftarrow \text{Skeleton_Evolution}(\{S_i\}_{i=1}^K, \{M_i\}_{i=1}^K)$

Given an input surface, which is represented by an unstructured triangular mesh M_Δ , see Figure 3 (a), first, in Phase 1, its patch layout is extracted by partitioning M_Δ into K patches M_i of 0-genus with one boundary, see Figure 3 (b). Then, in Phase 2, from the obtained partitioning (chartification) a topology-skeleton structure S is generated which consists of the joining of K surfaces S_i , each discretized by a quad grid, according to a given desired edge length h , see Figure 3 (c). In Phase 3 the topology-skeleton S is finally evolved towards the input triangulation M_Δ to create a pure quadrilateral mesh M_\square which accurately approximates the given 3D shape, see Figure 3 (d). In particular, in Phase 3 one of the following two evolution strategies can be applied: either evolve each skeleton part S_i separately as a surface with fixed boundary, or evolve the whole skeleton S as a single closed surface. Specific application contexts dictate which is the most convenient strategy to apply. This part of the thesis is based on the paper [1].

3.1 Evolution of the surface

Our aim is to prescribe the normal-direction evolution \mathbf{V}_N in (1) in such way that the evolving surface will be moving towards the given shape by a velocity field and the movement is smoothed by a mean curvature term. In order to control the trade-off between the advection and diffusion terms in , we introduce two functions $\epsilon(d(\mathbf{x}))$ and $\eta(d(\mathbf{x}))$ depending on the signed distance function $d(\cdot)$ at point \mathbf{x} , and define \mathbf{V}_N as

$$\mathbf{V}_N = \epsilon(d(\mathbf{x}))\Delta_{\mathbf{x}}\mathbf{x} + \eta(d(\mathbf{x}))\mathbf{N} , \quad (12)$$

where $d(\mathbf{x})$ represents the sign distance function to the given shape [?]. The sign distance function is defined to be positive inside the overall skeleton S and negative outside. The role of the coefficient $\epsilon(d(\mathbf{x}))$ in the diffusion term is to obtain stronger smoothing of the evolving surface in case $\mathbf{x}(\cdot)$ is far

from M_Δ ; therefore $\epsilon(d(\mathbf{x}))$ is defined by

$$\epsilon(d(\mathbf{x})) = c_1 \left(1 - e^{-\frac{d(\mathbf{x})^2}{c_2}} \right) \quad (13)$$

where c_1 and c_2 are parameters controlling the shape of $\epsilon(\cdot)$; in particular c_2 controls the transition width of the function, and c_1 controls its amplitude.

The function $\eta(d(\mathbf{x}))$ in (12) is given by

$$\eta(d(\mathbf{x})) = d(\mathbf{x}) \left(|-\nabla d(\mathbf{x}) \cdot \mathbf{N}| + \sqrt{1 - (\nabla d(\mathbf{x}) \cdot \mathbf{N})^2} \right). \quad (14)$$

The sign distance function $d(x)$ in (14) that multiplies the brackets, has two purposes. It accelerates the movement if the surface is far away from the triangulation and it flips the movement direction if it is outside of the triangulation. The first term in brackets represents the modification of (??). This term can be insufficient in case the normal vector \mathbf{N} and $\nabla d(\mathbf{x})$ are perpendicular. The second term in the brackets deals with this problem. It is the length of projection of $-\nabla d(\mathbf{x})$ onto the tangential plane. As a consequence it diminishes when $-\nabla d(\mathbf{x})$ is parallel to the normal vector of the surface \mathbf{N} and if $-\nabla d(\mathbf{x}) \perp \mathbf{N}$, then $\eta(d(\mathbf{x}))$ is proportional to the distance $d(\mathbf{x})$.

We utilize similar principles for discretization of the evolution equation as in previous chapter.

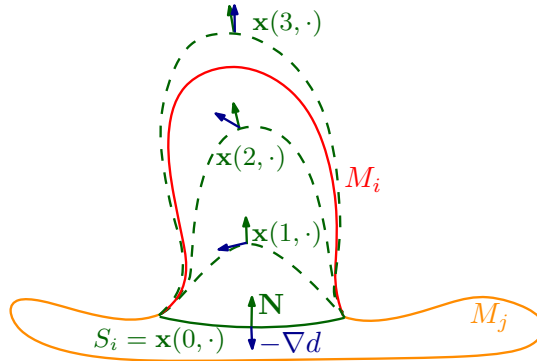


Figure 4: Illustrative example of (14) acting on $\mathbf{x}(t, \cdot)$ (green coloured lines) evolving towards a patch M_i , coloured in solid red. From bottom to top the different configurations of the vectors \mathbf{N} and $-\nabla d$ are shown at a point of the evolving surface $\mathbf{x}(t, \cdot)$ for $t = \{0, 1, 2, 3\}$.

3.2 Numerical experiments

We tested our approach on several input meshes. In general, we propose two approaches to the Skeleton Evolution Phase:

- **ALG_1** evolves each patch S_i of to the surface skeleton S separately, imposing Dirichlet boundary conditions at the common boundaries.
- **ALG_2** allows during the evolution to move jointly also the boundaries of each S_i , thus, allowing for better quad quality over the whole mesh as well as better vertex distribution around each S_i boundary.

The strategy **ALG_1** turns out to be useful when specific parts of the shape are aimed to be modified while maintaining the prescribed Phase 1 partitioning boundaries.

3.2.1 Example 2: Different resolutions

In this experiment, we produced the topology-skeletons S^h for `teddy` mesh using four different resolutions controlled by decreasing mesh size h in the range $\{0.05, 0.04, 0.025, 0.01\}$ and we evolved the associated skeletons. Then we have decreased the input M_Δ mesh resolution density down to 10%. The corresponding results are reported in Figure 5 in the first and last row while in the first column we plot the input triangulation.

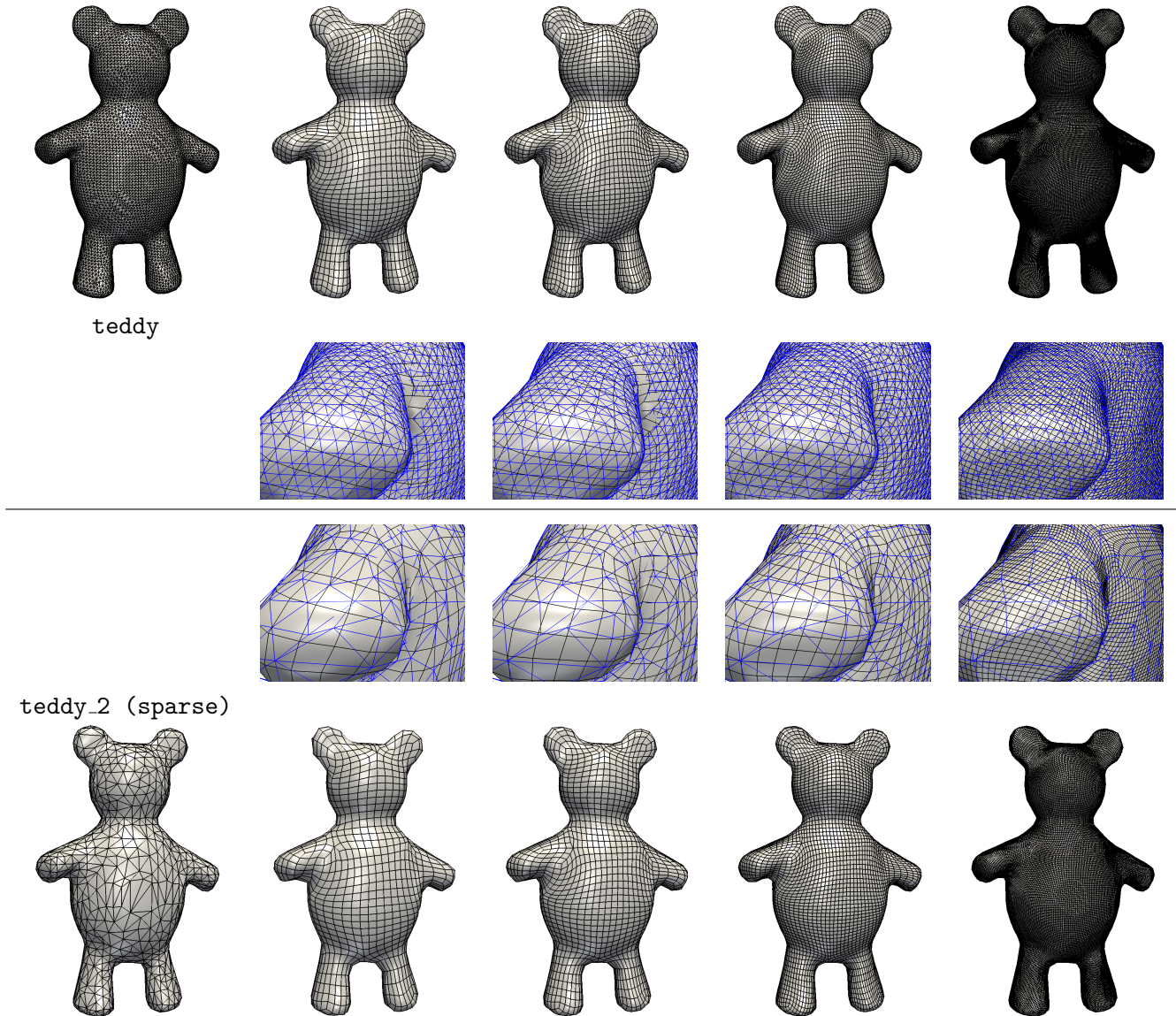


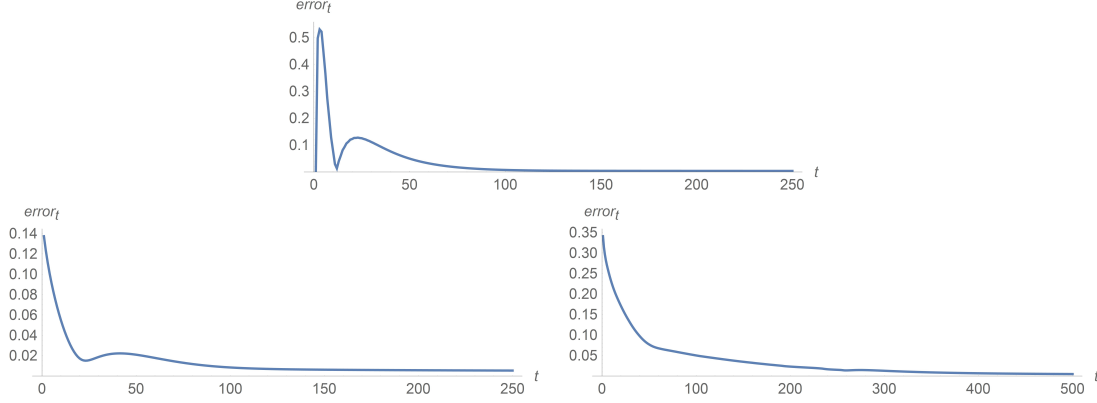
Figure 5: Example 2: Different resolution results for `teddy` mesh (top left) and its 90% down-sample (bottom left). From left to right the results for chosen parameter $h = \{0.05, 0.04, 0.025, 0.01\}$ respectively, together with zoom to the reconstructed mesh with original triangulation over-imposed in blue (second and third row).

From the reported results we can state that our algorithm is robust to the input-output mesh resolution, while its smoothness can be controlled by the parameters in ϵ function, relative to the diffusion term in the evolution model.

The corresponding Hausdorff distances in between results of Figure 5 are reported in Table 1.

Table 1: Example 2: Hausdorff distances between the results reported in Figure 5.

$d_H(M_\Delta, M_\square^h)$	h=0.040	h=0.025	h=0.010
teddy	22.600	12.783	3.014
teddy_2	22.680	13.577	5.796

Figure 6: A graph of $error_t$ for the experiments. Top: the evolving cylinder. Bottom left: the evolving hyperbolic paraboloid. Bottom right: the evolving dumbbell like surface.

4 Gaussian curvature based tangential redistribution

In this part we utilize the equation (6) to redistribute the point on the surface in depend to the Gaussian curvature. We present three numerical experiments. The first experiment has the initial condition in the shape of a cylinder. A decreasing $error_t$ for this evolution can be seen on Figure 6, top. The second experiment has an initial condition in the shape of a hyperbolic paraboloid $z = x^2 - y^2$. A decreasing $error_t$ for this evolution can be seen on Figure 6, left. Special case of an evolving surface is presented in the last experiment. The surface is closed, therefore there are is no boundary condition. The initial condition is a dumbbell like surface. A decreasing $error_t$ for this evolution can be seen on Figure 6, right.

5 Geodetic boundary value problem

The Earth's gravity field modelling is usually formulated in terms of the geodetic boundary value problems (GBVP) [2]. From the mathematical point of view, it represents an exterior oblique derivative BVP for the Laplace equation

$$-\Delta T(\mathbf{x}) = 0, \quad \mathbf{x} \in \Omega \subset \mathbf{R}^3, \quad (15)$$

$$v(\mathbf{x}) \cdot \nabla T(\mathbf{x}) = g(\mathbf{x}), \quad \mathbf{x} \in \Psi \subset \partial\Omega, \quad (16)$$

$$T(\mathbf{x}) = T_{Dir}(\mathbf{x}), \quad \mathbf{x} \in \partial\Omega - \Psi, \quad (17)$$

where $T(\mathbf{x})$ is the disturbing potential, the vector $v(\mathbf{x}) = \nabla U / |\nabla U|$ is an unit vector of the normal gravity, the region $\Psi \subset \partial\Omega$ represents the Earth topography. This part of the thesis is based on the paper [4].

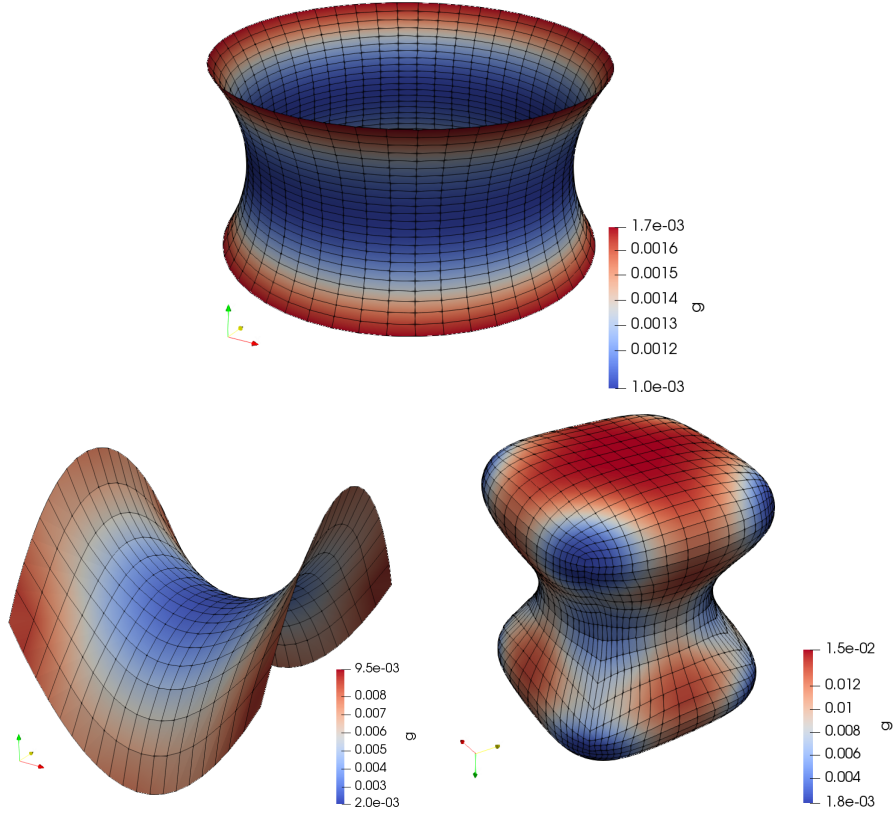


Figure 7: An evolving surfaces.

5.1 Discretization of oblique derivative BVP for Laplace equation

5.1.1 Approximation of the Laplace equation

We discretize the domain Ω by the regular hexahedron grid using the approach described in the first part of the thesis. Vertices of hexahedron are the representative points of finite volumes constructed later. Representative points are denoted by $\mathbf{x}_{i,j,k}$. Hexahedron finite volumes are constructed around inner (those that do not lie on the boundary $\partial\Omega$) representative points. We utilize a vertex centered finite volume method, i.e. the vertices of the finite volume lies in the average of the neighboring representative points.

Utilizing a Green's theorem we convert the Laplace equation to the integral of the normal derivative on the boundary of the finite volume. We reconstruct derivative in the normal direction \mathbf{n}_{ijk}^{pqr} by a derivatives in the directions \mathbf{s}_{ijk}^{pqr} , \mathbf{t}_{ijk}^{pqr} and \mathbf{f}_{ijk}^{pqr} .

$$\nabla T \cdot \mathbf{n}_{ijk}^{pqr} = \frac{1}{\beta_{ijk}^{pqr}} (\nabla T \cdot \mathbf{s}_{ijk}^{pqr} - \alpha_{ijk}^{pqr} \nabla T \cdot \mathbf{t}_{ijk}^{pqr} - \gamma_{ijk}^{pqr} \nabla T \cdot \mathbf{f}_{ijk}^{pqr}), \quad (18)$$

where \mathbf{s}_{ijk}^{pqr} is point connecting representative point and \mathbf{t}_{ijk}^{pqr} and \mathbf{f}_{ijk}^{pqr} are diagonal tangent vectors to the boundary, see Figure 8.

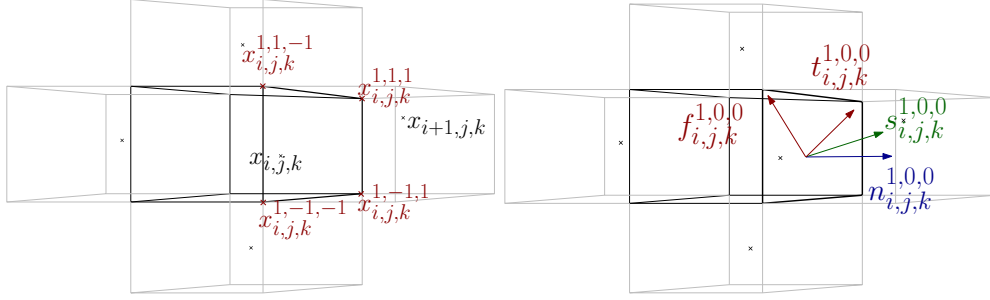


Figure 8: Finite volume

The equation resulting equation has a form

$$- \sum_{(p,q,r) \in N_1} m(e_{ijk}^{pqr}) \left(\frac{1}{\beta_{ijk}^{pqr}} \frac{T_{ijk} - T_{i+p,j+q,k+r}}{d_{ijk}^{pqr}} - \frac{\alpha_{ijk}^{pqr}}{\beta_{ijk}^{pqr}} \frac{T_{i,j,k}^{\oplus(p,q,r)} - T_{i,j,k}^{\ominus(p,q,r)}}{|\mathbf{x}_{i,j,k}^{\oplus(p,q,r)} - \mathbf{x}_{i,j,k}^{\ominus(p,q,r)}|} - \frac{\gamma_{ijk}^{pqr}}{\beta_{ijk}^{pqr}} \frac{T_{i,j,k}^{\boxplus(p,q,r)} - T_{i,j,k}^{\boxminus(p,q,r)}}{|\mathbf{x}_{i,j,k}^{\boxplus(p,q,r)} - \mathbf{x}_{i,j,k}^{\boxminus(p,q,r)}|} \right) = 0, \quad (19)$$

where $m(e_{ijk}^{pqr})$ is the area of the face e_{ijk}^{pqr} . Values $T_{i,j,k}^{\oplus(p,q,r)}$, $T_{i,j,k}^{\ominus(p,q,r)}$, $T_{i,j,k}^{\boxplus(p,q,r)}$ and $T_{i,j,k}^{\boxminus(p,q,r)}$ are values of unknown solution in the vertices of the finite volume. They are approximated as an average of values in the representative points.

5.1.2 Approximation of the oblique derivative boundary condition

We understand the equation (16) as advection equation, see [3], and we integrate it over the finite volume and utilizing a Green's theorem and constant approximation of solution on the finite volume an its boundary we obtain

$$\sum_{(p,q,r) \in N_1} T_{i,j,k}^{p,q,r} \int_{e_{i,j,k}^{p,q,r}} v \cdot \mathbf{n} \, ds - T_{i,j,k} \sum_{(p,q,r) \in N_1} \int_{e_{i,j,k}^{p,q,r}} v \cdot \mathbf{n} \, ds = m(V_{i,j,k})g, \quad (20)$$

where $T_{i,j,k}^{p,q,r}$ is the value on the boundary $e_{i,j,k}^{p,q,r}$ and $m(V_{i,j,k})$ is the volume of the finite volume $V_{i,j,k}$. The up-wind principle [3] is used in the sequel. Let us define the integrated flux over $e_{i,j,k}^{p,q,r}$ by

$$v_{i,j,k}^{p,q,r} = \int_{e_{i,j,k}^{p,q,r}} v \cdot \mathbf{n} \, ds. \quad (21)$$

If $v_{i,j,k}^{p,q,r} > 0$, $e_{i,j,k}^{p,q,r}$ is an outflow face. Thus $T_{i,j,k}^{p,q,r}$ should be computed by using the information from inside of the finite volume, $T_{i,j,k}^{p,q,r} := T_{i,j,k} + \nabla T_{i,j,k} \cdot (\mathbf{x}_{i,j,k}^{p,q,r} - \mathbf{x}_{i,j,k})$, where $\nabla T_{i,j,k}$ is an approximation of the gradient in the finite volume $V_{i,j,k}$. If $v_{i,j,k}^{p,q,r} < 0$, $e_{i,j,k}^{p,q,r}$ represents an inflow face, thus $T_{i,j,k}^{p,q,r}$ is computed using information from the neighbouring finite volume. Hence $T_{i,j,k}^{p,q,r} := T_{i+p,j+q,k+r} + \nabla T_{i+p,j+q,k+r} \cdot (\mathbf{x}_{i,j,k}^{p,q,r} - \mathbf{x}_{i+p,j+q,k+r})$.

Let us split the set N_1 for (i, j, k) into $N_1^{in}(i, j, k)$ and $N_1^{out}(i, j, k)$, where $N_1^{in}(i, j, k)$ are indexes of neighbours for which $v_{i,j,k}^{p,q,r} < 0$ and $N_1^{out}(i, j, k)$ are indexes of neighbours for which $v_{i,j,k}^{p,q,r} > 0$. Then the equation (20) becomes

Table 2: Statistics of residuals between our FVM solution and the EGM2008 in the domain above the Himalayas [m^2s^{-2}]

Resolution	$0.1^\circ \times 0.1^\circ \times 10km$	$0.05^\circ \times 0.05^\circ \times 5km$	$0.025^\circ \times 0.025^\circ \times 2.5km$
Grid density	$501 \times 301 \times 25$	$1001 \times 601 \times 49$	$2001 \times 1201 \times 97$
Min. value	-5.07	-1.68	-0.44
Mean value	1.79	0.87	0.33
Max. value	23.05	11.98	3.90
St. deviation	2.3	1.09	0.37

$$\sum_{(p,q,r) \in N_1} \left[(T_{i+p,j+q,k+r} + \nabla T_{i+p,j+q,k+r} \cdot (\mathbf{x}_{i,j,k}^{p,q,r} - \mathbf{x}_{i+p,j+q,k+r})) \min(0, v_{i,j,k}^{p,q,r}) \right. \\ \left. + (T_{i,j,k} + \nabla T_{i,j,k} \cdot (\mathbf{x}_{i,j,k}^{p,q,r} - \mathbf{x}_{i,j,k})) \max(0, v_{i,j,k}^{p,q,r}) - T_{i,j,k} v_{i,j,k}^{p,q,r} \right] = m(V_{i,j,k})g. \quad (22)$$

The gradient on the finite volume $V_{i,j,k}$ can be expressed using derivatives in three linear independent directions. Let us denote these directions \mathbf{p} , \mathbf{q} , \mathbf{r} . We reconstruct the gradient utilizing

$$\nabla T_{i,j,k} = \frac{\mathbf{p} \times \mathbf{q} \frac{\partial T}{\partial \mathbf{r}} + \mathbf{q} \times \mathbf{r} \frac{\partial T}{\partial \mathbf{p}} + \mathbf{r} \times \mathbf{p} \frac{\partial T}{\partial \mathbf{q}}}{\det(\mathbf{p}, \mathbf{q}, \mathbf{r})}. \quad (23)$$

5.2 Numerical experiments

In this section we present numerical experiments for the geodetic BVP (15)-(17). An experimental order of convergence is studied in the first two experiments. Next experiments present a reconstruction of a harmonic function on and above the complicated Earth's topography, namely over the Himalayas and in the area of Slovakia. The statistics of the Himalaya experiment compared with EGM2008 model can be seen in Table2

6 Advection equation

In this part we utilize the method from solving a GBVP and the input-implicit/output-explicit method [5] to solve a non-stationary advection equation. We propose an improved method that approximate the boundary of the finite volume more accurate, see Figure 10. For a smooth solutions we present a numerical experiment showing an improvement of the order of convergence from 1.6 to second order.

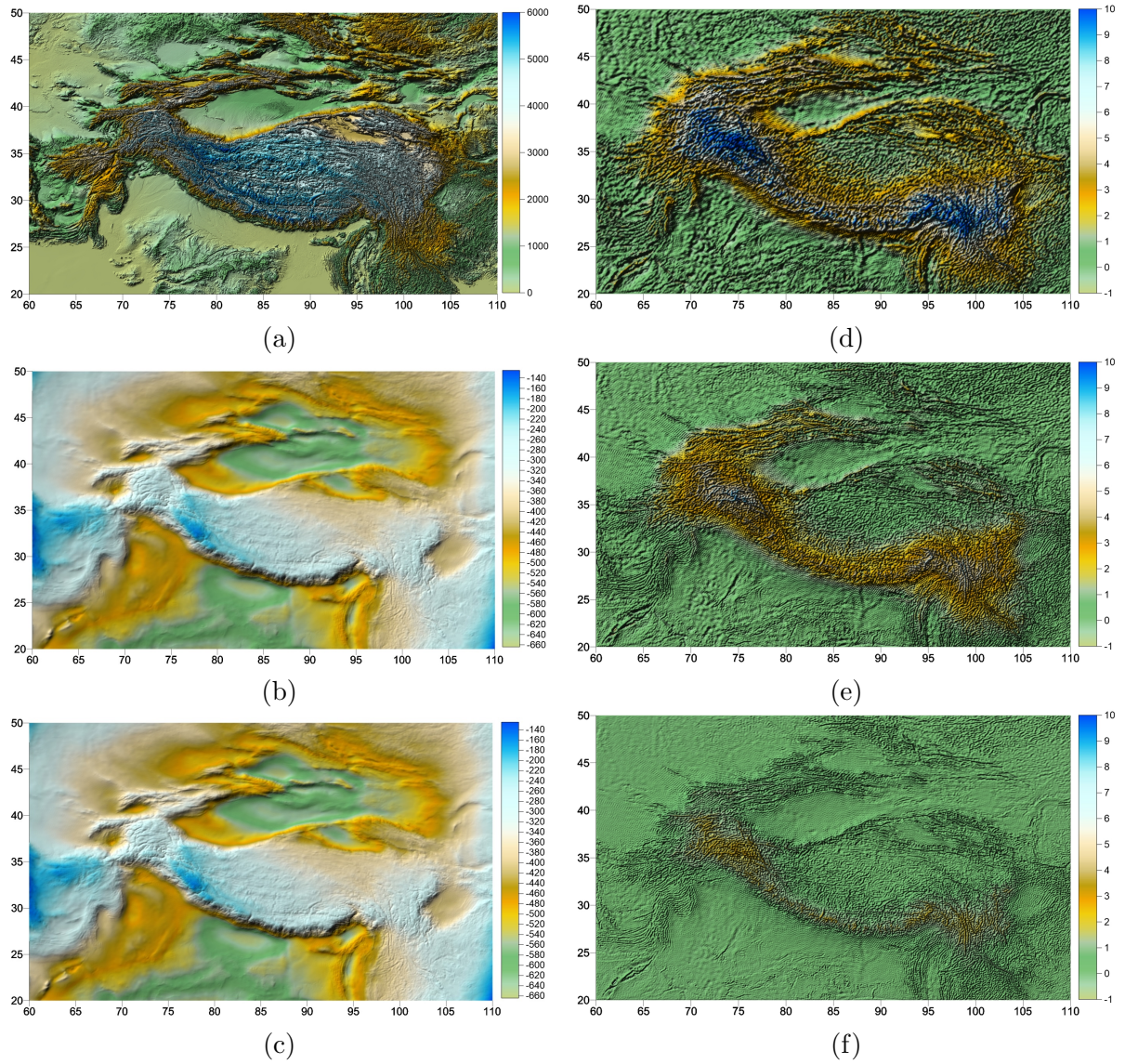


Figure 9: (a) The Earth's surface topography over the Himalayas (the bottom boundary) [m], (b) the disturbing potential from EGM2008 on the Earth's surface [$m^2 s^{-2}$], (c) the disturbing potential from our FVM solution [$m^2 s^{-2}$], (d, e, f) residuals between the EGM2008 and our FVM solution, where grid density is: (d) $501 \times 301 \times 25$, (e) $1001 \times 601 \times 49$, (f) $2001 \times 1201 \times 97$ points [$m^2 s^{-2}$].

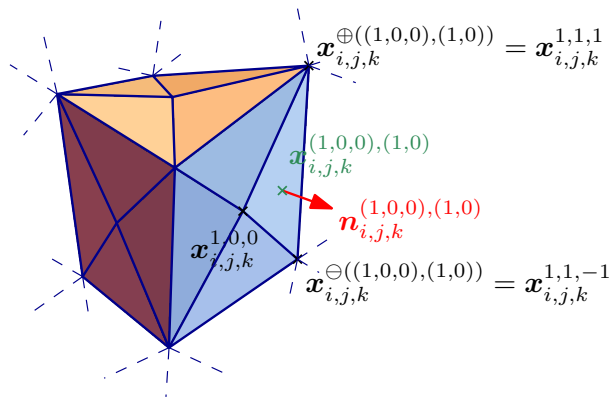


Figure 10: Illustration of a finite volume with boundaries split to the triangle boundaries

7 Conclusions

In the thesis we presented finite volume methods on non-uniform meshes for different applications. We presented methods for making quadrilateral and hexahedral meshes. Both methods use a surface evolution with a redistribution of points as primary tool. The chapter 2 deals with a construction of a 3D mesh over the Earth's topography by evolving a quadrilateral surface through the 3D domain. It involves a tangential redistribution of the evolving surface discretization points leading to a construction of a more regular non-uniform 3D hexahedron grid. We present a generation of pure quad semi-regular meshes built on a consistent object patch-layout. The resulting quad mesh respects the patch original layout. We shown that our method is robust for a different quality of input triangulated mesh. We also presented a method to redistribute points according to Gaussian curvature.

We presented a finite volume method for solving a geodetic boundary value problem and the advection equation in 3D domains. We have presented an original numerical method for solving the oblique derivative boundary value problem. The oblique derivative boundary condition has been treated as a stationary advection equation. We have introduced a discretization of the Laplace equation and oblique derivative boundary condition on grids constructed in the chapter 2. It consists of a reconstruction of the normal derivative to the finite volume using derivatives in the tangential directions. To treat numerically the oblique derivative BC as an advection equation, a new higher order up-wind method has been introduced for non-uniform grids. The presented numerical experiments have aimed to demonstrate efficiency of our proposed numerical method.

In the last chapter we introduced a finite volume method for the advection equation. We used ideas of the method from chapter 5 and IIOE strategy. Furthermore we propose a more accurate discretization method by splitting boundaries of the finite volumes to triangles. The numerical experiments show that this improved method is the second order of convergence for a solution without singularities. This method could be also incorporated in the solution GBVP to improve order of convergence.

References

- [1] M. Húska, M. Medl'a, K. Mikula, S. Morigi, Surface-Patch Quadrangulation, in preparation (2018)
- [2] K.R. Koch, A.J. Pope, Uniqueness and existence for the geodetic boundary value problem using the known surface of the earth, *Bull. Geod.*, 46, 467-476, (1972)
- [3] R.J. LeVeque, *Finite Volume Methods for Hyperbolic Problems*, Cambridge Texts in Applied Mathematics, ISBN: 978-0521009249, (2002)
- [4] M. Medl'a, K. Mikula, R. Čunderlík, M. Macák, Numerical solution to the oblique derivative boundary value problem on non-uniform grids above the Earth topography, *Journal of Geodesy*, Volume 92,
- [5] K. Mikula, M. Ohlberger, J. Urbán, Inflow-implicit/outflow-explicit finite volume methods for solving advection equations, *Applied Numerical Mathematics*, Volume 85, (2014), Pages 16-37, ISSN 0168-9274
- [6] K. Mikula, M. Remešiková, P. Sarkóci, D. Ševčovič, Manifold evolution with tangential redistribution of points, *SIAM J. Scientific Computing*, Vol. 36, No.4, pp. A1384-A1414 (2014)
- [7] H. Zhao, S. Osher, B. Merriman, M. Kang, Implicit and nonparametric shape reconstruction from unorganized data using a variational level set method, *Computer Vision and Image Understanding* 80 (2000) 295–319. doi:10.1006/cviu.2000.0875.

Zoznam publikačnej činnosti

ADC Vedecké práce v zahraničných karentovaných časopisoch

ADC01 MEDĽA, Matej - MIKULA, Karol - ČUNDERLÍK, Róbert - MACÁK, Marek. Numerical solution to the oblique derivative boundary value problem on non-uniform grids above the Earth topography. In *Journal of geodesy*. Vol. 92, no. 1 (2018), s. 1-19. ISSN 0949-7714. V databáze: CC: 000419971400001 ; SCOPUS ; DOI: 10.1007/s00190-017-1040-z.

AFC Publikované príspevky na zahraničných vedeckých konferenciách

AFC01 DANIEL, Patrik - MEDĽA, Matej - MIKULA, Karol - REMEŠÍKOVÁ, Mariana. Reconstruction of Surfaces from Point Clouds Using a Lagrangian Surface Evolution Model. In *Scale Space and Variational Methods in Computer Vision [elektronický zdroj] : proceedings, 5th International Conference, SSVM 2015*. Lège-Cap Ferret, France, 31. 5. - 4. 6. 2015. Switzerland : Springer, 2015, online, s. 589-600. ISBN 978-3319-18460-9.

AFD Publikované príspevky na domácich vedeckých konferenciách

AFD01 HÚSKA, Martin - MEDĽA, Matej - MIKULA, Karol - NOVYSEDLÁK, Peter - REMEŠÍKOVÁ, Mariana. A new form-finding method based on mean curvature flow of surfaces. In *ALGORITMY 2012 : 19th Conference on scientific computing. Proceedings*. Podbanské, SR, 9.-14.9.2012. Bratislava : Nakladateľstvo STU, 2012, s.120-131. ISBN 978-80-227-3742-5

AFD02 MEDĽA, Matej - MIKULA, Karol. Proof of second order convergence for the finite volume method on uniform grid for Laplace equation with Dirichlet boundary conditions. In *Advances in architectural, civil and environmental engineering [elektronický zdroj] : 25rd Annual PhD Student Conference on Architecture and Construction Engineering, Building Materials, Structural Engineering, Water and Environmental Engineering, Transportation Engineering, Surveying, Geodesy, and Applied Mathematics*. Bratislava, SR, 28. 10. 2015. 1. vyd. Bratislava : Slovenská technická univerzita v Bratislave, 2015, CD-ROM, s. 58-70. ISBN 978-80-227-4514-7.

AFD03 MEDĽA, Matej - MIKULA, Karol. New second order up-wind scheme for oblique derivative boundary value problem. In *ALGORITMY 2016 : 20th Conference on Scientific Computing. Proceedings of contributed papers and posters*. Podbanské, SR, 13. - 18. 3. 2016. 1. vyd. Bratislava : Slovak University of Technology, Faculty of Civil Engineering, 2016, S. 254-263. ISBN 978-80-227-4544-4.

AFD04 MEDĽA, Matej - MIKULA, Karol. Tvorba logicky štvoruholníkovej siete z mračna bodov. In *Advances in Architectural, Civil and Environmental Engineering [elektronický zdroj] : 26th Annual PhD Student Conference on Architecture and Construction Engineering, Building Materials, Structural Engineering, Water and Environmental Engineering, Transportation Engineering, Surveying, Geodesy, and Applied Mathematics*. 26. October 2016, Bratislava. 1. vyd. Bratislava : Slovenská technická univerzita v Bratislave, 2016, CD-ROM, s. 52-57. ISBN 978-80-227-4645-8.

- AFD05 MEDĽA, Matej - MIKULA, Karol. Tangenciálna redistribúcia bodov plochy závislá na krivosti. In Advances in Architectural, Civil and Environmental Engineering [elektronický zdroj] : 27th Annual PhD Student Conference on Applied Mathematics, Applied Mechanics, Geodesy and Cartography, Landscaping, Building Technology, Theory and Structures of Buildings, Theory and Structures of Civil Engineering Works, Theory and Environmental Technology of Buildings, Water Resources Engineering. 25. October 2017, Bratislava, Slovakia. 1. vyd. Bratislava : Spektrum STU, 2017, CD-ROM, s. 47-53. ISBN 978-80-227-4751-6.
- AFD06 MEDĽA, Matej - MIKULA, Karol. Gaussian curvature based tangential redistribution of points on evolving surfaces. In Proceedings of Equadiff 2017 Conference [elektronický zdroj] : July 24-28, 2017, Bratislava, Slovakia. 1. vyd. Bratislava : Spektrum STU, 2017, online, s. 255-264. ISBN 978-80-227-4757-8. V databáze: WOS: 000426796700029.

Štatistika: kategória publikačnej činnosti

ADC	Vedecké práce v zahraničných karentovaných časopisoch	1
AFC	Publikované príspevky na zahraničných vedeckých konferenciách	1
AFD	Publikované príspevky na domácich vedeckých konferenciách	6
AFG	Abstrakty príspevkov zo zahraničných konferencií	3
AFH	Abstrakty príspevkov z domácich konferencií	6
BFA	Abstrakty odborných prác zo zahraničných podujatí (konferencie...)	2
FAI	Redakčné a zostavovateľské práce knižného charakteru (bibliografie, encyklopédie, katalógy, slovníky, zborníky...)	1
Súčet		20

Článok v príprave

HÚSKA, Martin - MEDĽA, Matej - MIKULA, Karol - MORIGI, Serena, Surface-Patch Quadrangulation, in preparation (2018)